Machine Copy for Proofreading, Vol. x, y–z, 2007

EXTENDED CAVITY MODEL ANALYSIS OF STACKED CIRCULAR DISC

M. Mahajan, S. K. Khah, and T. Chakravarty

Department of Physics
Jaypee University of Information Technology
Waknaghat, Distt-Solan-173 215 (HP), India

Abstract—Stacked microstrip antennas deserve special attention due to their advantageous properties like dual frequency operation and wide bandwidth. In the present communication a theoretical model for single stacked microstrip disc antenna is proposed using extended cavity model. The method of analysis by this model is easier and intuitive than the full wave analysis. Single stacked microstrip disc antenna with co-axial feed locations at different radial positions is analyzed with this model taking different ratios of patch sizes. Antenna properties like return loss, input impedance, gain and radiation efficiency are calculated with the proposed model different cases and compared with the simulated and experimental results. The results are in fairly good agreement.

1. INTRODUCTION

Microstrip patch antennas are widely used antennas due to their many desirable features. However due to resonant behavior, the narrow bandwidth of the antennas is a concern. Stacking the antenna in multilayered configuration introduces additional resonance in the frequency resulting in the wide bandwidth and dual frequency operation. Stacked patch solution also presents many degrees of freedom (feeding point, gap between patches, dielectric constant etc.)

Several techniques have been appearing in the last years to improve the bandwidth and to have dual frequency operations in the microstrip antennas by stacking the microstrip antenna. Different methods were employed to analyze the stacked microstrip antenna like Method of Moments [1], Hankel Transform Domain Analysis [2], Coupled cavity methods [3], wave guide mode analysis [4] FDTD [5, 6]. These approaches were used for analysis of different types of microstrip

antennas [7, 8]. Apart from stacking the elements different techniques were employed to analyze microstrip antennas of different shapes for wide bandwidth or dual frequency techniques either by loading L-C-R circuit across a selective location in the disc via a thin shorting pin [9] or by T-strip loaded rectangular patch [10]. In the present article, a methodology is proposed by which the input impedance seen by a coaxial line feeding a probe exciting a stacked circular patch is evaluated for radial locations of feed probe. The outline of the method of evaluation of input impedance had been presented by De [11]. The expressions for the amplitudes of the excited fields in the resonant cavity are derived by taking the effect of wall admittance, dielectric loss and conductor loss into account. The expression for wall admittance has been derived following [12, 13]. The expression for electric field appearing in the formulation of input impedance is given as superposition of perturbed eigen-modes in the circular patch. The number of higher order modes used for computation is suitably truncated. Truncation however does not introduce any error in the computation of real value of input impedance. The radiation pattern for the loaded patch is evaluated by considering the magnetic current density at the electrical equivalent edge of the circular patch. Since the height of the substrate is very small and the current density is uniform along the z direction, we can approximate this by a filamentary magnetic current. The numerical and experimental results obtained by this model are compared with the simulated results and the results are fairly matching. The simulation is done by the Method of Moments based software IE3D which is commercially available.

2. THEORY

Consider a circular disk antenna with a radius r_1 and a thickness h, excited by a line current $I_0(z')$ on the feed pin. The feed pin has diameter d_f and is located at (r_0, ϕ_0) and the current density on the pin is given as $\vec{J}(r)$.

The input impedance of the antenna seen by a coaxial probe is given by [14]

$$Z_{in} = -\frac{1}{I_0^2} \int\limits_{S_0} \vec{E} \cdot \vec{J}^* dS \tag{1}$$

where the surface integral is over the feed pin surface S_0.

This expression for Z_{in} has been derived in [12] and is given as

$$Z_{in} = -\frac{1}{I_0^2} \sum_n \sum_p \frac{(j\omega + A)p_n^2}{(j\omega - C)(j\omega + A) + \omega_{np}^2} \tag{2}$$

where ω_{np} corresponds to the resonance of eigen-mode corresponding to TM_{np} mode. The parameters A & C are given as

$$A = Z_s \int_{se} |H_i|^2 dS \tag{3}$$

$$C = -Y_w \int_{sm} |E_i|^2 dS \tag{4}$$

where 'se' corresponds to top & bottom surfaces & 'sm' corresponds to side walls. Z_s and Y_w are the surface impedance of the conductor and wall admittance on the side walls, respectively. In expression (2), p_n is given as

$$p_n = \int_{s_0} E_i J^* dS$$

Since the current in the feed pin and fields in the patch radiator are uniform along z-axis, the above expression reduces to the form

$$p_n = \frac{I_0 h^2}{2\pi} \int_0^{2\pi} E_i \cdot d\beta \tag{5}$$

Consider the stacked circular patch configuration the geometry of the stacked patch is shown in Fig. 1.

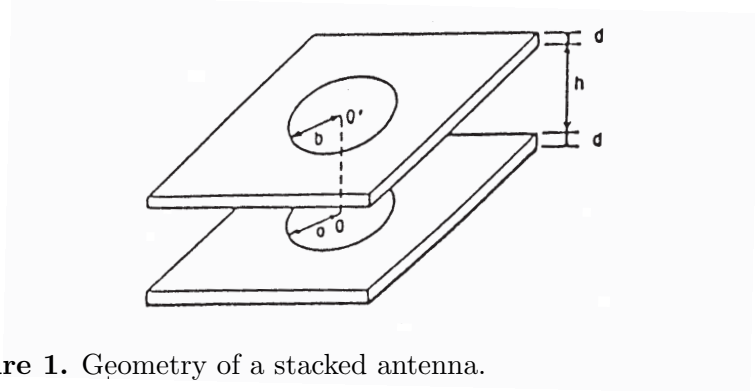

Figure 1. Geometry of a stacked antenna.

The Lower Circular Patch (LCP) of radius 'a' is loaded with Upper Circular Patch (UCP) of radius 'b' located on top of LCP with intermediate air gap of "h". The LCP radiator is excited by coaxial probe of diameter d_f. The expression (2) is used for evaluation of input impedance. The use of the expression requires evaluation of normal mode fields. The normal mode fields are evaluated by

assuming $Y_W = 0$. While formulating the basic theory concerning the computation of input impedance around a given resonant frequency f_{np} corresponding to the excited mode TM_{np}, it is important to differentiate the notations for wave propagation constant. These are given as below.

$$\begin{aligned} k &= \omega\sqrt{\mu_0\varepsilon_0\varepsilon_{eff}} \text{ for measurement frequency } f = f_{np} \pm \Delta f. \\ k_{np} &= \omega_{np}\sqrt{\mu_0\varepsilon_0\varepsilon_{eff}} \end{aligned}$$

and

$$k_0 = \omega\sqrt{\mu_0\varepsilon_0}$$

For thin microstrip antenna $(h/\lambda_g < 0.02)$, $\varepsilon_{eff} \cong \varepsilon_r$

In Region I (LCP), the expressions for electric field and magnetic field are given as

$$E_z = -j\omega_{np}\mu C_n^{(1)} F_n^{(1)}(k \cdot r)\cos n\phi \tag{6}$$

$$H_r = -(n/r)C_n^{(1)} F_n^{(1)}(k \cdot r)\sin n\phi \tag{7}$$

and

$$H_\phi = -k_{np} C_n^{(1)} F_n^{(1)'}(k \cdot r)\cos n\phi \tag{8}$$

where

$$C_n^{(1)} \text{ is a constant}$$
$$F_n^{(1)}(k_{np}r) = J_n(k \cdot r)$$

and

$$F_n^{(1)'}(k_{np}r) = J_n'(k \cdot r)$$

For such cases, application of boundary condition leads to

$$Jn'(k_{np}a) = 0$$

Application of the boundary condition gives the resonant frequency.

In order to evaluate the constant $C_n^{(1)}$, the normalization condition [15] is used.

$$\int_V \varepsilon |E|^2 dV = 1$$

For the entire volume the normalization condition for the problem under consideration assumes the form

$$\int_0^h \int_0^{2\pi} \int_0^a \varepsilon |E_z|^2 r dr = 1$$

From this

$$C_n^{(1)} = \frac{1}{k} \cdot \sqrt{\frac{1}{\pi h \mu [I_1]}} \tag{9}$$

In Eq. (9)

$$I_1 = \int_0^a J_n^2(k \cdot r) r dr$$

The different parameters appearing in expression for input impedance (2) for the problem under consideration assumes the following form.

$$A = Z_s \int_0^{2\pi} \int_0^a \left\{ |H_\phi|^2 + |H_r|^2 \right\} r dr \tag{10}$$

where surface resistance Z_s is given as

$$Z_s = \left\{ \frac{\pi f \mu}{\sigma} \right\}^{\frac{1}{2}}$$

and

$$C = -Y_w \int_0^h \int_0^{2\pi} |E_z|^2 r d\phi dz$$
$$\text{at } r = a \tag{11}$$

From this

$$A = Z_s \pi {C_n^{(1)}}^2 \left[k^2 I_3 + n^2 I_4 \right]. \tag{12}$$

where

$$I_3 = \int_0^a J_n^{2'}(k \cdot r) r dr$$

$$I_4 = \int_0^a \frac{J_n^2(k \cdot r)}{r^2} r dr$$

The expression of "A" corresponds to the copper loss in the microstrip.

Consider a loaded microstrip patch radiator excited by a coaxial line feeding a probe located at $(r_0, \phi_0, 0)$.

Using the transformation [16]

$$r = r_0 + \frac{d_f}{2} \cos \beta$$

and expanding the Bessel function in Taylor series, the function $F_n^{(1)}(k \cdot r)$ is obtained as

$$F_n^{(1)}(k \cdot r) = J_n(k \cdot r_0) + \frac{k \cdot d_f}{2} J_n'(k \cdot r_0) \cos\beta \tag{13}$$

where the higher order terms of the Taylor series expansion are neglected.

Using the transformation

$$\phi = \frac{d_f}{2r_0} \sin\beta$$

and expanding $\cos(n\phi)$ & $\sin(n\phi)$ in series of Bessel function it is found

$$\cos(n\phi) = J_0\left(\frac{nd_f}{2r_0}\right) + 2\sum_{q=1}^{\infty} J_{2q-1}\left(\frac{nd_f}{2r_0}\right)\cos(2q\beta) \tag{14}$$

$$\sin(n\phi) = 2\sum_{q=1}^{\infty} J_{2q-1}\left(\frac{nd_f}{2r_0}\right)\sin[(2q-1)\beta] \tag{15}$$

substituting in Eq. (5) and carrying out the integration

$$p_n = -j\omega\mu h I_0 C_n^{(1)} J_n(k \cdot r_0) J_0\left(\frac{nd_f}{2r_0}\right) \tag{16}$$

substituting Eq. (16) in Eq. (2), we get

$$Z_{in} = \mu^2 h^2 \sum_n \sum_p \frac{(j\omega + A) C_n^{(1)^2} \omega^2 \left[J_n(k \cdot r_0) J_0\left(\frac{nd_f}{2r_0}\right)\right]^2}{(j\omega - A)(j\omega + A) + \omega_{np}^2} \tag{17}$$

3. FORMULATION OF COMPUTATION OF RADIATION PATTERN

The magnetic current density evaluated at the electrical equivalent edge r_e of the circular patch can be written as

$$\vec{M}_s = -2\hat{n} \times E_z|_{\rho'=re} \tag{18}$$

Since the height of the substrate is very small and the current density given by (18) is uniform along the z-direction, we can approximate (18) by a filamentary magnetic current of

$$I_m = h\vec{M}_s = \hat{a}_\phi 2h(-j\omega\mu) C_n^{(1)} F_n^{(1)}(k \cdot r_e)\cos(n\phi) \tag{19}$$

In the far-field the total $\vec{E}$ fields can be written as [17]

$$E_r = 0 \tag{20}$$

$$E_\vartheta \cong -jk_0\frac{e^{-jk_0r}}{4\pi r}L_\phi \tag{21}$$

$$E_\phi \cong +jk_0\frac{e^{-jk_0r}}{4\pi r}L_\vartheta \tag{22}$$

where

$$L_\phi = \iint\limits_S M_\phi\cos(\phi-\phi')e^{+jk_0r'\cos\Psi}ds' \tag{23}$$

$$L_\vartheta = \iint\limits_S M_\phi\cos\vartheta\sin(\phi-\phi')e^{+jk_0r'\cos\Psi}ds' \tag{24}$$

In Eqs. (23) & (24)

$$r'\cos\Psi = \rho'\sin\vartheta\cos(\phi-\phi')$$
$$ds' = \rho'd\rho'd\phi'$$

Using the following two relations

$$\int\limits_0^{2\pi}\cos(\phi'-\phi)e^{jm\phi'}e^{jk\rho'\sin\vartheta\cos(\phi'-\phi)}d\phi'$$
$$= \pi j^m e^{jm\phi}\left\{j\left[J_{m+1}(k\rho'\sin\vartheta)-J_{m-1}(k\rho'\sin\vartheta)\right]\right\}$$

and

$$\int\limits_0^{2\pi}\sin(\phi'-\phi)e^{jm\phi'}e^{jk\rho'\sin\vartheta\cos(\phi'-\phi)}d\phi'$$
$$= \pi j^m e^{jm\phi}\left[J_{m+1}(k\rho'\sin\vartheta)+J_{m-1}(k\rho'\sin\vartheta)\right]$$

we obtain for TM_{11} mode

$$E_\vartheta = -\frac{e^{-jk_0r}}{r}\left(\frac{h}{\pi}\right)\left(\frac{\omega\mu_0}{\sqrt{\varepsilon_r}}\right)C_n^{(1)}\left[J_0(k_0r_e\sin\vartheta)-J_2(k_0r_e\sin\vartheta)\right]\{\cos\phi\} \tag{25}$$

and

$$E_\phi = +\frac{e^{-jk_0r}}{r}\left(\frac{h}{\pi}\right)\left(\frac{\omega\mu_0}{\sqrt{\varepsilon_r}}\right)C_n^{(1)}\cos\vartheta$$
$$\times\left[J_0(k_0r_e\sin\vartheta)+J_2(k_0r_e\sin\vartheta)\right]\{\sin\phi\} \tag{26}$$

3.1. Radiated Power

The power radiated by a shorted patch is estimated as

$$P_r = \frac{1}{2\eta_0} \int_0^{2\pi} \int_0^{\pi/2} \left(|E_\vartheta|^2 + |E_\phi|^2 \right) r^2 \sin\vartheta d\vartheta d\phi \tag{27}$$

For TM_{11} mode expression (27) can be rewritten as

$$P_r = \frac{2\pi}{\eta_0} \left(\frac{E_0}{k_0 r_e} \right)^2 \left[(k_0 r_e)^2 I_7 + I_8 \right] \tag{28}$$

where

$$\begin{aligned} \eta_0 &= 120\pi \\ E_0 &= \frac{h}{\pi} \left(\frac{\omega\mu_0}{\sqrt{\varepsilon_r}} \right) C_n^{(1)} \\ I_7 &= \int_0^{\pi/2} \left[J_1'(k_0 r_e \sin\vartheta) \right]^2 \sin\vartheta d\vartheta \\ I_8 &= \int_0^{\pi/2} \left[J_1(k_0 r_e \sin\vartheta) \right]^2 \frac{(\cos\vartheta)^2}{\sin\vartheta} d\vartheta \end{aligned}$$

4. EVALUATION OF WALL ADMITTANCE Y_W

In order to determine the input impedance of the loaded circular patch, it is necessary to take into account the reactive power due to the electric and magnetic stored energy in the fringe of the disk and the real power due to radiation. These reactive and active powers are given by equivalent boundary admittance at the disk edge.

The boundary admittance Y_W is given by [18, pp. 107–109]

$$Y_W = g_n + jb_n \tag{29}$$

where

$$g_n = \frac{P_T}{\frac{1}{2} \int_{S_m} |E_z|^2 ds|_{\rho=r_e}} \tag{30}$$

and

$$b_n = \frac{-P_i}{\frac{1}{2}\int\limits_{S_m} |E_z|^2 ds|_{\rho=r_e}} \tag{31}$$

where P_i is the reactive power & P_T is the total power given by the following set of expressions

$$P_T = P_r + P_c + P_d$$

where P_r is the radiated power, P_c and P_d are the copper loss and dielectric loss respectively. P_c is same as "A" and the dielectric loss is given as

$$P_d = \frac{1}{2} h\omega\varepsilon_r\varepsilon_0 \tan\delta\pi(\omega\mu)^2 C_n^{(1)^2}[I_1]$$

Thus

$$g_n = \frac{h}{\eta_0 r_e}\left[(k_0 r_e)^2 I_7 + I_8\right] \cdot \frac{1}{eff_{np}} \tag{32}$$

where eff_{np} is the efficiency of the antenna when TM_{np} mode is excited and is given as

$$eff_{np} = \frac{P_r}{P_T} \tag{33}$$

Estimation of the reactive power, is made by computing the fields at the edge of the disk Substituting, we get the expression for b_n

$$b_n = \frac{1}{\eta_0}\frac{\varepsilon_0\varepsilon_r\omega\pi r_1^2}{h}\left[\left\{1 + \frac{2h}{\pi r_1\varepsilon_r}\left(\ln\left(\frac{\pi r_1}{2h}\right) + 1.7726\right)\right\}^{1/2} - 1\right] \tag{34}$$

Using Eqs. (32) and (34), one can compute Y_W.

From expression (34), it is evident that wall susceptance accounts for the fringing fields which increases the physical radius to an effective radius r_e. It is important to note that while computing the input impedance around resonance, the resonant frequency ω_{np} is to be given as input value. This "ω_{np}" already accounts for the fringing field using r_e as the effective radius of the patch. Therefore, to avoid multiple corrections due to fringing fields, $\mathbf{b_n}$ **is taken to be zero**.

In general, since the substrate height is small compared to the wavelength, it can be assumed that the fringing field is extended up to a distance from the edges so a magnetic wall can be set at that region. The effective radius can be calculated as follows.

$$\Delta C_{LCP} = \ln\left(\frac{a}{2h}\right) + 1.41\varepsilon_r + 1.7726 + \frac{h}{a}(0.286\varepsilon_r + 1.65) \tag{35}$$

$$r_e = a\sqrt{1 + \frac{2h}{\pi a\varepsilon_r}\Delta C_{LCP}} \tag{36}$$

The electric and magnetic energies stored inside the lower cavity becomes

$$W_e = \frac{P_d}{2\omega \tan\delta} \tag{37}$$

and

$$W_h = \frac{1}{4}\mu_0 h \frac{P_c}{R_s} \tag{38}$$

5. APPLICATION OF END-CORRECTION NETWORK OF A COAXIAL PROBE

The theory developed in the previous sections for a shorting post loaded circular microstrip antenna assumes the use of a coaxial probe. For validating this theory through experimental verification, it is necessary to properly model the coaxial probe. A survey of analytical models used for evaluating the input impedance of probe-fed microstrip antenna is given in reference [19]. In the present work, for purpose of computing input impedance, the end-correction network suggested by Zheng et al. [20] is used. Zheng suggests that TEM aperture field approximation can provide an accurate result of input admittance, and there is no need to introduce a specific correction network for most applications. Constant current probe model is valid only when both $k_1 d \ll 1$ and $a'/d \ll 1$ are satisfied (where d is the substrate height and a' is the radius of the centre conductor of the coaxial probe). An end-correction network consisting of a series inductor and a shunt capacitance should be used for higher accuracy. Using this correction network the input impedance for the probe-fed microstrip antenna is given as

$$Y_{TEM} \approx \frac{1}{[R_p + j\omega(L_p + L_0)]} + j\omega C_0 \tag{39}$$

where

$$\begin{aligned} C_0 &= \varepsilon_0\varepsilon_r \left[6d\ln^2(b'/a')\right]^{-1} \left\{3\pi\left[b'^2 - a'^2 - 2b^2\ln(b'/a')\right]\right. \\ &\quad \left. +4\pi h^2 \ln(b'/a') - 12h^3(\pi^2 b')^{-1}\cdot X_0\right\} \end{aligned} \tag{40}$$

where

$$\begin{aligned} X_0 &= \xi(3) - \sum_{n=1}^{\infty} n^{-3}\exp\left[-2n\pi(b'-a')/h\right] \\ L_0 &= -\mu_0 h k_1^2 \left[4\pi\ln(b'/a')\right]^{-1}\cdot\left[(b'^2 + a'^2)\ln(b'/a') - b'^2 + a'^2\right] \\ &\quad \times \left[\ln(k_1 a'/2) + \gamma\right] \end{aligned} \tag{41}$$

the Riemann zeta function and $\xi(3) = 1.202$ and b' is the radius of the outer conductor of the probe.

The $R_p + j\omega L_p$ in (39) is the same input impedance derived from the constant current probe approximation. The end-correction network formed by C_0 and L_0 can be used even when the input impedance Z_p associated with the infinite parallel plates is replaced with that of a finite size patch when the probe is not located very close to the edge.

The expression for input impedance resembles the form of a parallel RLC circuit, although in this case each element can be considered as frequency dependent.

Based on the analogy with a parallel resonant circuit the input impedance for a probe free circular patch can also be re-written as

$$Z_{in} = \frac{1}{\dfrac{2P_T}{|V|^2} + j\dfrac{4\omega}{|V|^2}W_e - j\dfrac{4\omega}{|V|^2}W_h} \tag{42}$$

where

$$V = -dE_{av}$$

and

$$E_{av} = \frac{1}{2d}\int_0^{2\pi} E_z^2(r_1, \phi)d\phi$$

6. THEORY OF STACKED CIRCULAR PATCH

The cavity model developed for a single circular patch (LCP) can now be extended for a stacked geometry. In this case the stacked antenna has to be considered as two coupled cavities. It is necessary to accurately predict the upper and lower cavity resonant frequency; next the electric fields generated inside the upper and lower cavities are added together using the correct effective values of the dielectric constant.

The Green's function is obtained for the LCP and the UCP. The main difference lies in the effective dielectric constants and the patch dimensions. The resulting total electric field inside the cavities can be calculated by adding together the contributions of the field in the superstrate and in the substrate. This assumption can be supported by the fact that the cavity model assumes no "z" variations of the electric field. The assumption gets invalidated if the height of the superstrate is large as compared to wavelength.

The lower cavity can be considered to be loaded by a dielectric material, ignoring the upper patch. This is valid since the fields are

concentrated between the lower patch and the ground. The superstrate on the other hand will alter the effective dielectric constant. However in the present case there is a substantial air-gap between the substrate and the superstrate. For this case exact computation of effective dielectric constant is not necessary since height of air-gap$\gg d$. If the air-gap is reduced, it will be necessary to replace ε_r by $\varepsilon_{r,eff} = p \cdot \varepsilon_r$ where "p" is an empirical correction factor less than one.

The upper patch can be considered in isolation as uncoupled cavity with an air gap. For such the expression for effective dielectric constant is given as [21]

$$\varepsilon_{re} = \frac{\varepsilon_r(1 + h/d)}{(1 + \varepsilon_r h/d)} \tag{43}$$

where h is the air-gap and d is the superstrate height.

The resonant frequency is obtained from

$$f_{np} = \frac{\chi_{np} \cdot 300}{2\pi b_{eff}\sqrt{\varepsilon_{ef}}} \tag{44}$$

where

$$\varepsilon_{ef} = \frac{4\varepsilon_{re}\varepsilon_{r,dyn}}{\left(\sqrt{\varepsilon_{re}} + \sqrt{\varepsilon_{r,dyn}}\right)^2} \tag{45}$$

Here

$$\varepsilon_{r,dyn} = \frac{C_{dyn}(\varepsilon = \varepsilon_0\varepsilon_{re})}{C_{dyn}(\varepsilon = \varepsilon_0)} \tag{46}$$

where C_{dyn} is the dynamic capacitance defined as

$$C_{dyn} = C_{0,dyn} + C_{\varepsilon,dyn} \text{ (main and fringing capacitances)} \tag{47}$$

The dynamic capacitances are related to static capacitances as

$$C_{0,dyn} = 0.3525 C_{0,stat} \tag{48}$$

$$C_{0,dyn} = (1/2) C_{\varepsilon,dyn} \tag{49}$$

The static capacitances are evaluated as follows.

$$C_{0,stat} = \left(\varepsilon_0\varepsilon_{re}\pi b^2\right)/h_T \tag{50}$$

Here $h_T = d + h + d =$ The total height over the ground plane

$$\begin{aligned} C_{\varepsilon,stat} &= C_{0,stat} \cdot q \\ q &= u + v + uv \\ u &= \frac{1 + \varepsilon_{re}}{\varepsilon_{re}} \frac{4}{\pi b/h_T} \end{aligned} \tag{51}$$

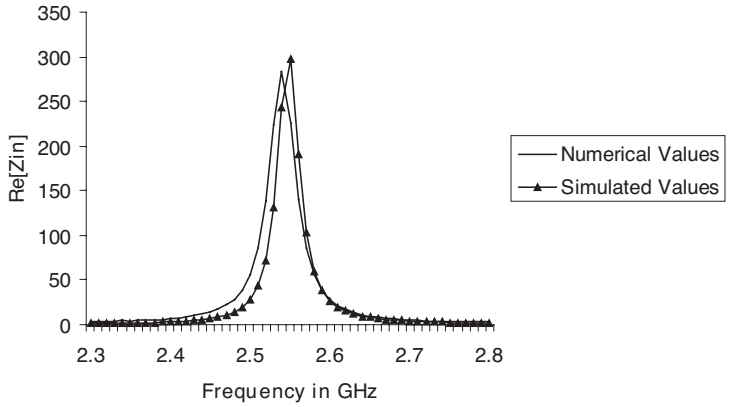

Figure 2. Variation of real input impedance $\{\mathrm{Re}[Z_{in}]\}$ with frequency for single patch $r_0 = 20\,\mathrm{mm}$.

$$\begin{aligned} v &= \frac{2}{3t}\left(\frac{\ln(p)}{8+\pi b/h_T}\right)+\left(\frac{1}{t}-1\right)/g \\ t &= 0.37+0.63\varepsilon_{re} \\ p &= \frac{1+0.8(b/h_T)^2+(0.31b/h_T)^4}{1+0.9b/h_T} \\ g &= 4+2.6b/h_T+2.9h_T/b \end{aligned}$$

The effective radius of the microstrip disk is

$$b_{eff} = b\sqrt{1+m\cdot q} \tag{52}$$

The upper patch has to be analyzed like an uncovered microstrip patch. However lower patch does not provide sufficient ground plane and this fact will introduce errors. The effects of coupling between the substrate and the superstrate will change the effective dimensions of the upper ring and thus will increase the resonant frequency as compared to the case without substrate. It is necessary to accurately account for the interaction between fringing fields in the lower and the upper patch by changing the effective radii of the upper patch.

Once the effective dielectric constant is obtained for the upper patch, the effective dimension r_{2eff} is obtained. Here "m" is an empirical correction factor.

Next, the input impedance of upper patch with probe location on the edge is obtained using expression (42) with suitable changes in the various parameters. Thus each cavity is studied separately as

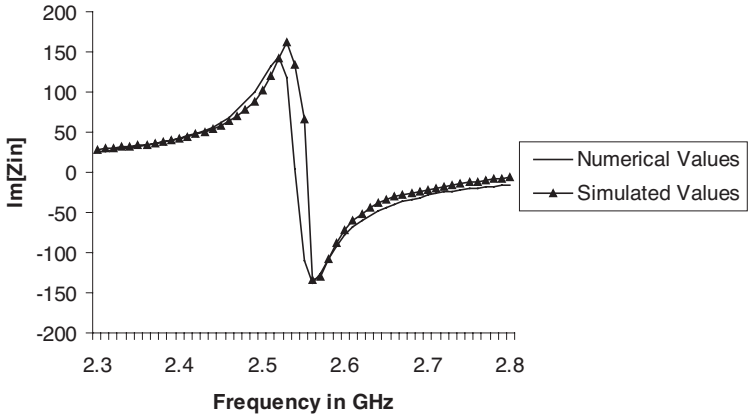

Figure 3. Variation of imaginary input impedance $\{\mathrm{Im}[Z_{in}]\}$ with frequency for single patch $r_0 = 20\,\mathrm{mm}$.

though they are uncoupled. The coupling is done through mutual capacitance between the two patches. Since impedance of each cavity is obtained using normalized voltage of 1 V, the coupled impedance is again normalized to 1 V by considering half of impedance value obtained using expression (42).

Though the resonance of the cavities is studied in uncoupled mode, the radiated fields are strongly coupled. Therefore in the formulation mentioned above, P_r remains a single expression taking into account both the uncoupled fields.

7. RESULTS

For designing of broadband antenna, the stacked approach is being considered using the present model. The stacked antenna consists of a circular patch of a radius "a" on the lower substrate of dielectric thickness "d" & dielectric constant ε_r. Another circular patch of radius "b" is placed on top of the lower patch on identical dielectric with an air gap of "h" between these two. With the help of present model different radiation properties of the stacked antenna are analyzed. For numerical calculation and simulation of the antenna input parameters taken are $a = 22.65\,\mathrm{mm}$, $d = 0.787\,\mathrm{mm}$, $h = 9\,\mathrm{mm}$ and the ratio of patch sizes $b/a = 1$, 1.05, and 1.1.

In this paper, the problem of stacked patch is considered as two uncoupled impedances coupled through capacitive coupling. To demonstrate the accuracy of the proposed model, the theoretical and

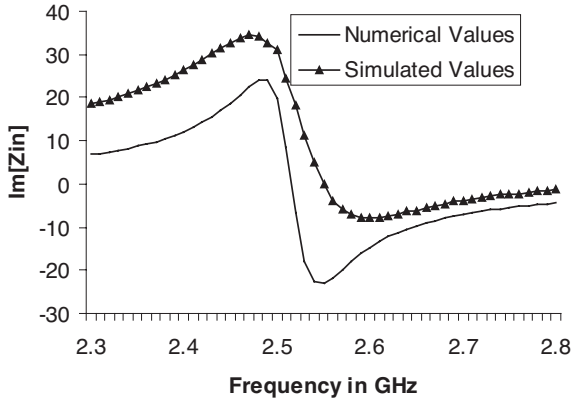

Figure 4. Variation of $\mathrm{Im}[Z_{in}]$ with frequency for the ratio of patch sizes $b/a = 1$ and $r_0 = 12\,\mathrm{mm}$.

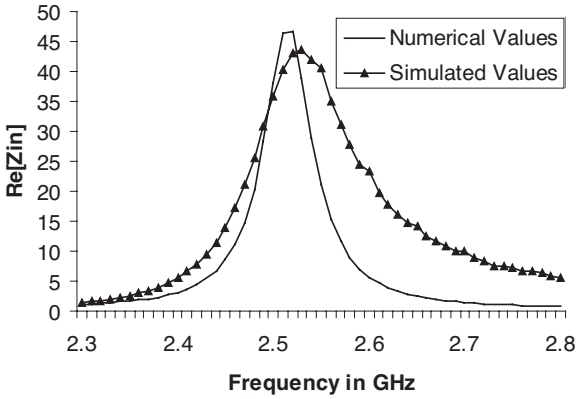

Figure 5. Variation of $\mathrm{Re}[Z_{in}]$ with frequency for the ratio of patch sizes $b/a = 1$ and $r_0 = 12\,\mathrm{mm}$.

simulated impedances are compared for single LCP.

It is seen that very good agreement is observed in the resonant frequency as well as magnitudes of impedances. Now the UCP is placed and the problem is both numerically solved and compared with simulated results. The following figures [Fig. 4–Fig. 11] display the real and imaginary part of input impedances for $b = 1.1a$ & $b = a$ and feed point location (r_0) at 12 mm and 20 mm along the radial direction. This model is suitable for computation when the height is taken to be lower than proposed. As the value of $\frac{h}{\lambda_0} > 0.02$ the cavity

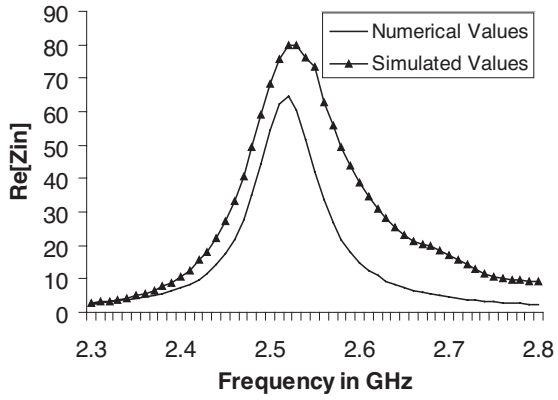

Figure 6. Variation of $\mathrm{Re}[Z_{in}]$ with frequency for the ratio of patch sizes $b/a = 1$ and $r_0 = 20\,\mathrm{mm}$.

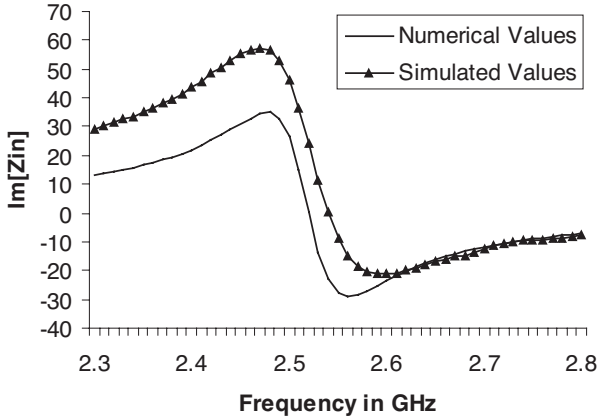

Figure 7. Variation of $\mathrm{Im}[Z_{in}]$ with frequency for the ratio of patch sizes $b/a = 1$ and $r_0 = 20\,\mathrm{mm}$.

model starts failing. However since the measurement result showed an enhanced bandwidth at $h = 9\,\mathrm{mm}$, the same was used for comparison.

The error percentage of resonant frequency for both cases of $b = a$ and $b = 1.1a$ is reported in Table 1. In case of $b = 1.1a$, there is a disagreement to the extent of 4% in resonant frequency. While as in case of $a = b$ the disagreement in the resonant frequency is less than 1.5%. This is due to the fact that LCP which is acting as ground plane for UCP is not fully covering UCP. Also cavity model exhibits error

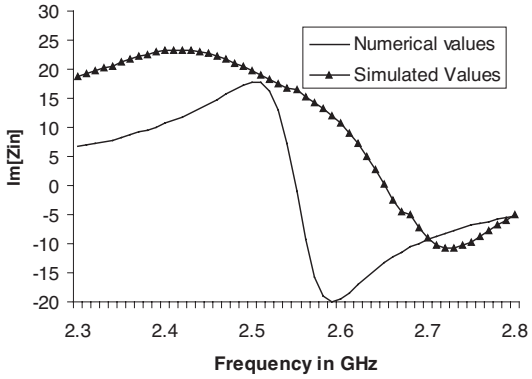

Figure 8. Variation of $\mathrm{Im}[Z_{in}]$ with frequency for the ratio of patch sizes $b/a = 1.1$ and $r_0 = 12\,\mathrm{mm}$.

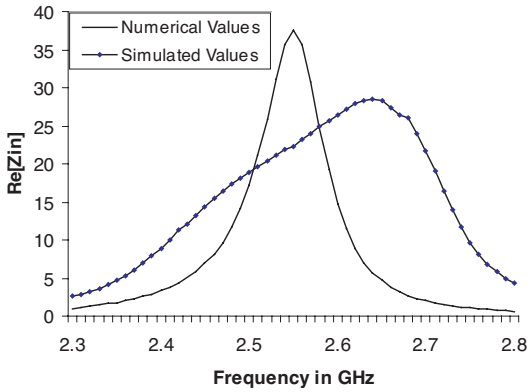

Figure 9. Variation of $\mathrm{Re}[Z_{in}]$ with frequency for the ratio of patch sizes $b/a = 1.1$ and $r_0 = 12\,\mathrm{mm}$.

when height of substrate is thick as in this case.

Now an edge fed stacked antennas is fabricated for dimensions $a = 22.65\,\mathrm{mm}$, $h = 9\,\mathrm{mm}$, $d = 0.787\,\mathrm{mm}$ and $b = 1.05a$ and is tested. Fig. 12 shows the result. With these values the resultant structure exhibits input impedance of 50 ohms (characteristic impedance of feed line). While in absence of stacked element the input impedance is nearly 270 ohms. The band width in this case is found 200 MHz around the central frequency of 2.6 GHz.

The theory is applied to single patch with dimensions $a = 22.65\,\mathrm{mm}$ and $r_0 = 12\,\mathrm{mm}$ and to the stacked elements of dimensions

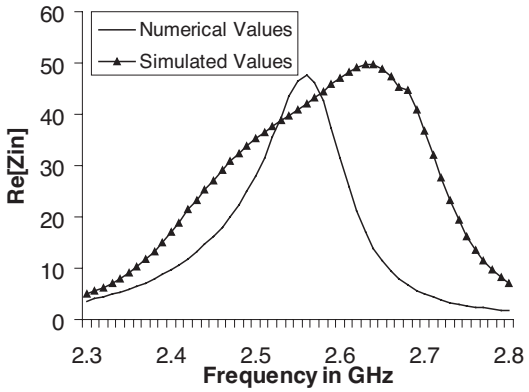

Figure 10. Variation of $\mathrm{Re}[Z_{in}]$ with frequency for the ratio of patch sizes $b/a = 1.1$ and $r_0 = 20\,\mathrm{mm}$.

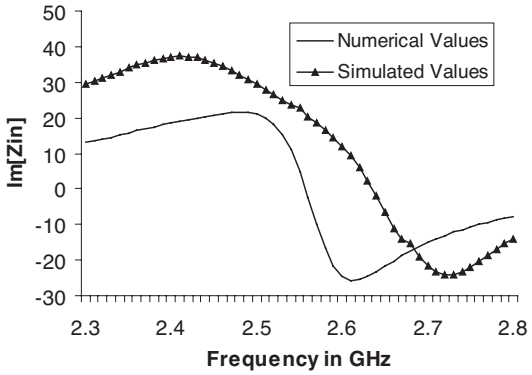

Figure 11. Variation of $\mathrm{Im}[Z_{in}]$ with frequency for the ratio of patch sizes $b/a = 1.1$ and $r_0 = 20\,\mathrm{mm}$.

Table 1. Percentage error in resonant frequency for the ratio of patch size $b/a = 1.1$ and $b/a = 1$ for $r_0 = 12\,\mathrm{mm}$ and $20\,\mathrm{mm}$.

Ratio of b/a	Radial feed point location	Percentage error in Resonant Frequency
1	r_o=12 mm	1.17
	r_o=20 mm	0.78
1.1	r_o=12 mm	3.77
	r_o=20 mm	2.66

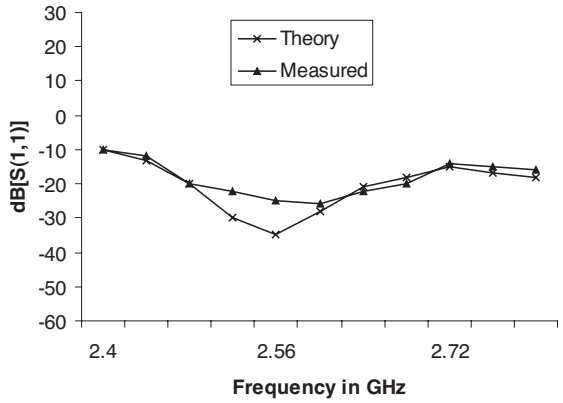

Figure 12. Theoretical and measured return loss for a single element stacked antenna.

Table 2. Comparison of gain of stacked patch and single patch antenna.

Antenna Type	Frequency in GHz	Gain in dB
Single Patch (Radial feed at 12 mm)	2.51	2.93
	2.55	5.03
	2.56	5.23
	2.62	3.20
Stacked Patch (Radial Feed at 12 mm and b/a=1)	2.51	7.72
	2.55	8.26
	2.62	8.11

$a = 22.65\,\text{mm}$, $r_0 = 12\,\text{mm}$ and $b = a$. It is observed that with the stacking of elements input impedance is considerably reduced to the feed line impedance (50 ohms) or near it. For this case, the band size observed is 2.51 GHz–2.62 GHz around central frequency of 2.55 GHz. In case of patch antenna it is at 2.56 GHz. Comparison of gain of patch and stacked antenna is calculated numerically Table 1.

It is evident from the table that gain is considerably high in case of stacked elements even at the edges of the band width. Numerical and simulated values of the radiation efficiency are reported in Table 3. In both cases the efficiency is more than 94% and is in good agreement.

Table 3. Numerical and Simulated values of radiation efficiency of stacked antenna with radial feed ($r_0 = 12\,\text{mm}$ and ratio of patch size $b/a = 1$).

Antenna	Frequency in GHz	Radiation Efficiency in Percentage	
		Numerical	Simulated
Stacked Patch	2.51	97.75	94.20
	2.55	97.80	94.25
	2.62	97.42	94.16

8. CONCLUSION

In this article the authors present a theoretical model based on analytical techniques for computing the impedance of stacked circular microstrip antenna around fundamental resonance for a probe fed case. The result for an edge-fed case show 10% bandwidth is achievable. The results with feed point location at different radial positions also predict not only the enhancement of bandwidth but improvement in the radiation characteristics of stacked antenna. A major application for such antenna is the ease with which a circular polarized array can be designed with large bandwidth, For some applications it is required to have two closely spaced resonances for transmit and receive mode with circular polarization. For such applications, this antenna is very suitable along with a microstrip diplexer for T_x and R_x isolation.

REFERENCES

1. Tulintseff, A. N. and R. M. Sorbello, "Current and radiation fields of electromagnetically coupled microstrip antennas," *IEEE AP-S,* Vol. 2, 928–931, 1987.
2. Fan, Z. and K. F. Lee, "Hankel transform domain analysis of a dual frequency stacked circular disk and annular ring microstrip antennas," *IEEE Trans. Antennas Propag.,* Vol. 39, 867–870, 1991.
3. Cock, R. T. and C. G. Christodoulou, "Design of a two-layer capacitively coupled, microstrip patch antenna element for broadband applications," *IEEE Antennas Propag. Soc. Int. Symp. Dig.,* Vol. 2, 936–939, 1987.
4. Shen, Z. and R. H. MacPbie, "Waveguide model analysis of single and stacked probe-fed microstrip antenna with circular

geometries," *IEEE Antennas Propag Symposium,* Vol. 2, 598–601, 1998.

5. Nishiyama, E. and M. Aikawa, "Wide band and high gain microstrip antenna with thick parasitic patch substrate," *IEEE Antennas Propag Society International Symposium,* Vol. 1, 273–276, 2004.
6. Nishiyama, E., M. Aikawa, and Egashira, "FDTD analysis of stacked microstrip antenna with high gain," *Progress In Electromagnetics Research*, PIER 33, 29–43, 2001.
7. Tagle, J. G. and C. G. Christodoulou, "Extended cavity model analysis of stacked microstrip ring antenna," *IEEE Trans. Antennas Propag.,* Vol. 45, No. 11, 1628–1637, 1997.
8. Anguera, J., C. Puente, C. Borja, N. Delbene, and J. Soler, "Dual frequency broad band stacked microstrip patch antenna," *IEEE Antenna and Wireless Letters,* Vol. 3, 36–39, 2003.
9. Chakravarty, T., S. M. Roy, S. K. Sanyal, and A. De, "A novel microstrip patch antenna with large impedance bandwidth in VHF/UHF range," *Progress In Electromagnetics Research* PIER 54, 83–93, 2005.
10. Gao, S., L. W. Li, and A. Sambell, "FDTD analysis of dual frequency microstrip patch antenna," *Progress In Electromagnetics Research*, PIER 54, 155–178, 2005.
11. De, A., "Studies on rectangular and circular patch radiators," Ph.D. Thesis, Indian Institute of Technology, Kharagpur, 1985.
12. Shen, L. C., "Analysis of the circular-disk printed-circuit antenna," *IEEE Proc. Microw. Antennas Propag.,* Vol. 126, 1220–1222, 1979.
13. Yano, S. and A, Ishimaru, "A theoretical study of the input impedance of a circular microstrip disk antenna," *IEEE Trans. Antennas Propag.,* Vol. AP-29, 77–83, 1981.
14. Collin, R. E. and F. J. Zucker, *Antenna Theory,* Part I, McGraw-Hill, 1969.
15. Harrington, R. F., *Time Harmonic Electromagnetic Fields,* McGraw-Hill, NY, 1961.
16. Yano, S. and A. Ishimaru, "A theoretical study of the input impedance of a circular microstrip disk antenna," *IEEE Trans. Antennas Propag.,* Vol. AP-29, 77–83, 1981.
17. Balanis, C. A., *Antenna Theory: Analysis and Design,* 2nd edition, Chap. 14, John Wiley, New York, 1997,
18. Bahl, I. J. and P. Bhartia., *Microstrip Antennas,* Artech House, Deldham, MA, 1980.

19. Damiano, J. P. and A. Papiernik, "Survey of analytical and numerical models for probe-fed microstrip antennas," *IEEE Proc. Microwave Antennas Propag.,* Vol. 141, No. 1, 15–21, Feb. 1994.
20. Zheng, J. X. and D. C. Chang, "End-correction network of a coaxial probe for microstrip patch antennas," *IEEE Trans. Antennas Propag.,* Vol. AP-39, No. 1, 115–118, 1991.
21. Guha, D., "Resonant frequency of circular microstrip antenna with or without air gaps," *IEEE Trans. Antennas Propag.,* Vol. AP-49, No. 1, 55–59, Jan. 2001.